

Dalton Transactions

Accepted Manuscript



This is an *Accepted Manuscript*, which has been through the Royal Society of Chemistry peer review process and has been accepted for publication.

Accepted Manuscripts are published online shortly after acceptance, before technical editing, formatting and proof reading. Using this free service, authors can make their results available to the community, in citable form, before we publish the edited article. We will replace this *Accepted Manuscript* with the edited and formatted *Advance Article* as soon as it is available.

You can find more information about *Accepted Manuscripts* in the [Information for Authors](#).

Please note that technical editing may introduce minor changes to the text and/or graphics, which may alter content. The journal's standard [Terms & Conditions](#) and the [Ethical guidelines](#) still apply. In no event shall the Royal Society of Chemistry be held responsible for any errors or omissions in this *Accepted Manuscript* or any consequences arising from the use of any information it contains.

Catalytic Behaviour in the Ring-Opening Polymerisation of Organoaluminiums Supported by Bulky Heteroscorpionate Ligands

Jose A. Castro-Osma,^a Carlos Alonso-Moreno,^b Agustín Lara-Sánchez,^a *Antonio Otero,^{a,*} Juan Fernández-Baeza,^a Luis F. Sánchez-Barba,^a Ana M. Rodríguez^c.

⁵ Received (in XXX, XXX) Xth XXXXXXXXX 200X, Accepted Xth XXXXXXXXX 200X

First published on the web Xth XXXXXXXXX 200X

DOI: 10.1039/b000000x

A series of alkyl organoaluminium complexes based on bulky heteroscorpionate ligands were designed as catalysts for the ring-opening polymerisation of cyclic esters. Thus, treatment of AlX₃ (X = Me, Et) with bulky acetamide or thioacetamide heteroscorpionate ligands nbptamH (1) [nbptamH = *N*-naphthyl-2,2-bis(3,5-dimethylpyrazol-1-yl)thioacetamide], fbpamH (2) [fbpamH = *N*-fluorenyl-2,2-bis(3,5-dimethylpyrazol-1-yl)acetamide], ptbptamH (3) [ptbptamH = *N*-phenyl-2,2-bis(3,5-di-*tert*-butylpyrazol-1-yl)thioacetamide], ntbptamH (4) [ntbptamH = *N*-naphthyl-2,2-bis(3,5-di-*tert*-butylpyrazol-1-yl)thioacetamide], ptbpamH (5) [ptbpamH = *N*-phenyl-2,2-bis(3,5-di-*tert*-butylpyrazol-1-yl)acetamide] and (*S*)-mtbpamH (6) [(*S*)-mtbpamH = (*S*)-(-)-*N*- α -methylbenzyl-2,2-bis(3,5-di-*tert*-butylpyrazol-1-yl)acetamide] for 1 hour at 0 °C afforded the dialkyl aluminium complexes [AlX₂{ κ^2 -nbptam}] (X = Me 7, Et 8), [AlX₂{ κ^2 -fbpam}] (X = Me 9, Et 10), [AlX₂{ κ^2 -ptbptam}] (X = Me 11, Et 12), [AlX₂{ κ^2 -ntbptam}] (X = Me 13, Et 14), [AlX₂{ κ^2 -ptbpam}] (X = Me 15, Et 16) and [AlX₂{ κ^2 -(*S*)-mtbpam}] (X = Me 17, Et 18). The structures of the complexes were determined by spectroscopic methods and the X-ray crystal structure of 14 was also established. The alkyl-containing aluminium complexes 7–18 can act as efficient single-component initiators for the ring-opening polymerisation of ϵ -caprolactone and *rac*-lactide. The polymerisations are living, as evidenced by the narrow polydispersities of the isolated polymers and the linear nature of the number average molecular weight versus conversion plot. Finally, a comparative study of the ring-opening polymerisation for the new bulky heteroscorpionate aluminium initiators and the less congested aluminium analogues is reported.

Introduction

Concern about environmental problems and the depletion of fossil fuel feedstocks have encouraged industrial and academic research groups to search for environmentally friendly and renewable materials as an alternative to the increasingly less attractive polyolefins.¹ Over the last decade, Ring-Opening Polymerisation (ROP) of bio-renewable cyclic esters has attracted the most attention in this respect.² Whereas tin(II) 2-ethylhexanoate has led the industrial production of this kind of biopolymer in this methodology, drawbacks such as the difficulty in controlling the properties of the resulting products and the inherent toxicity of heavy metals such as tin remain as limitations that must be overcome.³ These issues are already being circumvented by the introduction of well-defined metallic initiators for the controlled ROP of cyclic esters through a coordination-insertion mechanism.² A plethora of aluminium,⁴ alkaline and alkaline earth,⁵ lanthanide⁶ and other initiators⁷ supported by a judicious selection of ancillary ligands have been reported in the literature. Of these systems, aluminium catalysts can be considered as a workable proposition as this is the most abundant metal on earth, the catalysts are low-cost, have low toxicity, high Lewis acidity, and they

are redox-inactive in nature.⁸ In fact, these entities already play a key role in catalysis for the transformation of small organic molecules,⁹ as co-catalysts in the polymerisation of olefins,¹⁰ and for the synthesis of cyclic carbonates.¹¹

A good initiator for the ROP of cyclic esters requires a redox-inactive metal, an inert inorganic template L_nM, and a polar metal-ligand bond that can undergo an insertion reaction with C–X multiple bonds. Taking all these considerations into account, we have contributed widely to this field in recent years by designing new heteroscorpionate ligands related to the bis(pyrazol-1-yl)methane system and incorporating several pendant donor arms bearing an anionic functional donor group to prepare metal-based initiators for the ROP of cyclic esters.¹² Some years ago, we focused on the design of alkyl organoaluminium entities in order to study their synthetic accessibility, structural arrangements and catalytic behaviour in the ROP of ϵ -caprolactone (ϵ -CL) and lactide (LA).¹³ In this context, to the best of our knowledge very few alkyl complexes without a cocatalyst have been reported as successful initiators for the ROP of cyclic esters.¹⁴

In a previous study^{13c} we carried out the facile synthesis and full characterisation of several organoaluminium entities based on acetamide and

thioacetamidate ancillary ligands in $\kappa^2\text{NO}$ and $\kappa^2\text{NN}$ coordination modes, respectively. $\varepsilon\text{-CL}$ and LA were polymerised by these entities to give linear medium molecular weight polymers with moderate-to-broad polydispersities. Unfortunately, appreciable levels of selectivity were not obtained in the polymerisation of *rac*-LA. During our studies we realised that a dynamic exchange process in which an intramolecular associative displacement of one pyrazolyl group for another was taking place in the organoaluminium initiators, and this 'swinging event' could interfere with biopolymer productivities. In fact, a relevant interdependency between activities in the ROP of $\varepsilon\text{-CL}$ and estimated exchange constants (k_{ex}) was observed; a decrease of k_{ex} was shown to correlate with increasing productivity in the ROP.

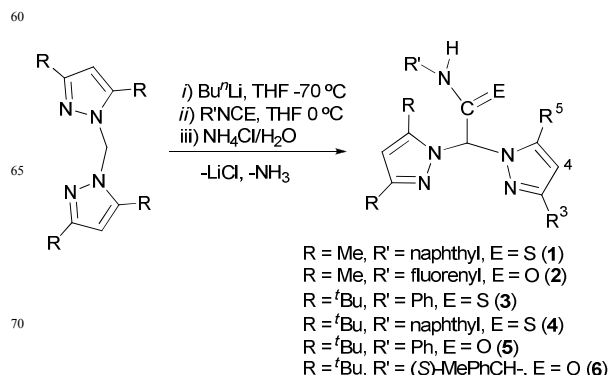
The aim of the work described here was to prepare efficient organoaluminium initiators based on bulky heteroscorpionate ligands in an effort to achieve increased activity in ROP and, assuming chain-end control, to exert better control of the polymer microstructure than their previously reported counterparts.^{13c} The use of these new entities as good single-component living initiators for the polymerisation of $\varepsilon\text{-CL}$ and *rac*-LA under well-controlled conditions is discussed in detail and an analysis of the polymer microstructures is provided.

Results and Discussion

Synthesis and structural characterisation

The performance of initiators in terms of activity, productivity, degree of control and stereoselectivity depends crucially on the ancillary ligands, which define the steric and electronic environment around the active metal centre. In an effort to increase the steric hindrance around the metal centre of the organoaluminium initiators, six new heteroscorpionate ligand precursors bearing more sterically encumbered substituents were designed and synthesised according to literature procedures.^{6e,15} The bulkiness was imposed either in the pyrazole groups or in the acetamidate/thioacetamidate moiety. Thus, the one-pot reaction of bis(3,5-dimethylpyrazol-1-yl)methane (bdmpzm)¹⁶ or bis(3,5-di-*tert*-butylpyrazol-1-yl)methane (bdtbpmz)¹⁶ with Bu^nLi , followed by the addition of a series of isocyanates [fluorene-2-yl, phenyl or (*S*)-(-)- α -methylbenzyl isocyanates] and isothiocyanates (phenyl and naphthyl isothiocyanates) and then saturated aqueous ammonium chloride solution, afforded the desired compounds nbptamH (1), fbpmamH (2), ptbptamH (3), ntbptamH (4), ptbpmamH (5) and (*S*)-mtbpmamH (6), which were isolated in good yields (ca. 80%) after the appropriate workup (Scheme 1). Compound 6 was isolated as an enantiopure ligand precursor. For compounds 1–6 there are three possible tautomers (see Fig. S1 in ESI†). The ¹H NMR spectra of these compounds all contain a broad singlet between δ 6.00 and 13.00 ppm (see Fig. S2 in ESI†), which corresponds to the N–H group of the acetamide or thioacetamide moieties and indicates the

presence of only one tautomer in solution (depicted in Scheme 1). The different acetamide or thioacetamide compounds were characterised spectroscopically (see Experimental Section).



Scheme 1. Synthesis of compounds 1–6.

The structural disposition of this tautomer was confirmed by X-ray crystal structure determination for 3 and 5 (see Fig. 1). The crystallographic data and selected interatomic distances and angles are given in Tables S1 and S2 in ESI†. The pyrazole rings of this compound are oriented in a quasi-antiparallel disposition with respect to each other, presumably to minimise intramolecular steric interactions between the N(2) and N(4) atoms of the two rings.

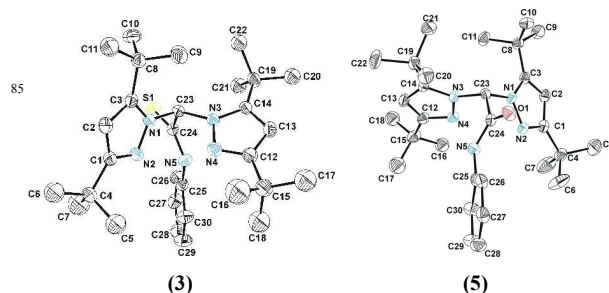
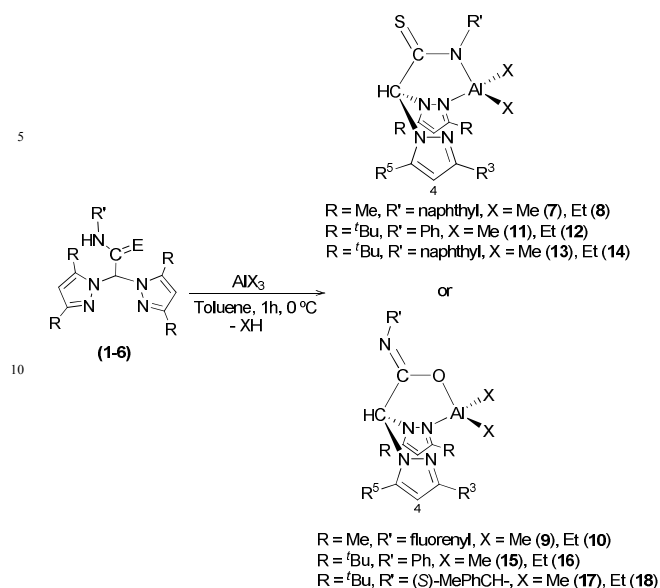


Fig. 1. ORTEP drawings of compounds 3 and 5. Thermal ellipsoids are set at 30% probability and hydrogen atoms are omitted for clarity.

Protonolysis reactions of heteroscorpionate protio-precursors 1–6 with one equivalent of AlX_3 in a 1:1 molar ratio in toluene at 0 °C gave the mononuclear dialkyl aluminium complexes [$\text{AlX}_2\{\kappa^2\text{-nbptam}\}$] ($\text{X} = \text{Me}$ 7, Et 8), [$\text{AlX}_2\{\kappa^2\text{-fbpam}\}$] ($\text{X} = \text{Me}$ 9, Et 10), [$\text{AlX}_2\{\kappa^2\text{-ptbptam}\}$] ($\text{X} = \text{Me}$ 11, Et 12), [$\text{AlX}_2\{\kappa^2\text{-ntbptam}\}$] ($\text{X} = \text{Me}$ 13, Et 14), [$\text{AlX}_2\{\kappa^2\text{-ptbpmam}\}$] ($\text{X} = \text{Me}$ 15, Et 16) and [$\text{AlX}_2\{\kappa^2\text{-(S)-mtbpmam}\}$] ($\text{X} = \text{Me}$ 17, Et 18), with elimination of the corresponding alkane (see Scheme 2).^{13,14a} Compounds 7–18 were isolated as white or yellow solids in good yields after the appropriate workup procedure (see Experimental Section). Complexes 17 and 18 were isolated as mixtures of two diastereoisomers in similar proportions.



Scheme 2. Synthetic route to compounds 7–18.

The different acetamidate and thioacetamidate compounds were characterised spectroscopically (see Experimental Section). The ¹³C NMR signals of the carbonyl or thiocarbonyl groups in these complexes are good indicators of the bonding mode of the acetamidate or thioacetamidate moieties of the ligands.^{13a,c} The acetamidate carbon resonances, RNCO, were shifted to higher field with respect to those of the neutral ligands, indicating that the acetamidate moieties were coordinated to the aluminium centre through the O atom (see Scheme 2). In contrast, the corresponding signal for the thioacetamidate carbon resonance, RNCS, is shifted to lower field with respect to that in the neutral ligand (see Experimental Section), indicating that the thioacetamidate moiety is coordinated to the metal centre through the N atom. However, a small amount of delocalised E–C–N bond probably exists in the acetamidate or thioacetamidate moieties of the heteroscorpionate ligands. The ¹H and ¹³C-¹H NMR spectra for compounds 7–14 at room temperature show broad resonances for some of the protons and carbons (see Fig. 2a), indicating the existence of fluxional behaviour (see Fig. S3, variable temperature ¹H NMR spectra for compound 14 in toluene-d₈), which is thought to be due to exchange processes between coordinated and noncoordinated pyrazole rings (‘swinging events’). This type of fluxional process was observed in the aluminium counterparts.^{13c} The bulkiness imposed in the new organoaluminium derivatives bearing ^tBu₂-pyrazole seems to slow, at room temperature, the ‘swinging event’ previously observed for the Me₂-pyrazole counterparts^{13c} (see Fig. S3) and for complexes 15–18 the exchange process between coordinated and noncoordinated pyrazole rings does not take place at all. Thus, for complexes 17 and 18, which bear a chiral heteroscorpionate ligand, the ¹H NMR spectra at room

temperature shows double signals due to the two diastereoisomers present (see Fig. 2b). It is worth noting that, given the coordination mode of the ligands, all of the complexes are chiral regardless of the existence of a chiral centre in the heteroscorpionate ligand used as the scaffold. NOESY-1D NMR experiments were carried out in order to confirm the assignment of most ¹H NMR resonances and ¹H-¹³C heteronuclear correlation (*g*-HSQC) experiments allowed the resonances corresponding to some carbons of the pyrazole rings and alkyl groups to be assigned. The spectroscopic data support a tetrahedral disposition for the aluminium atom with a κ²NN coordination mode of the thioacetamidate heteroscorpionate ligand, whereas the acetamidate derivatives have a κ²NO coordination mode, as depicted in Scheme 2.

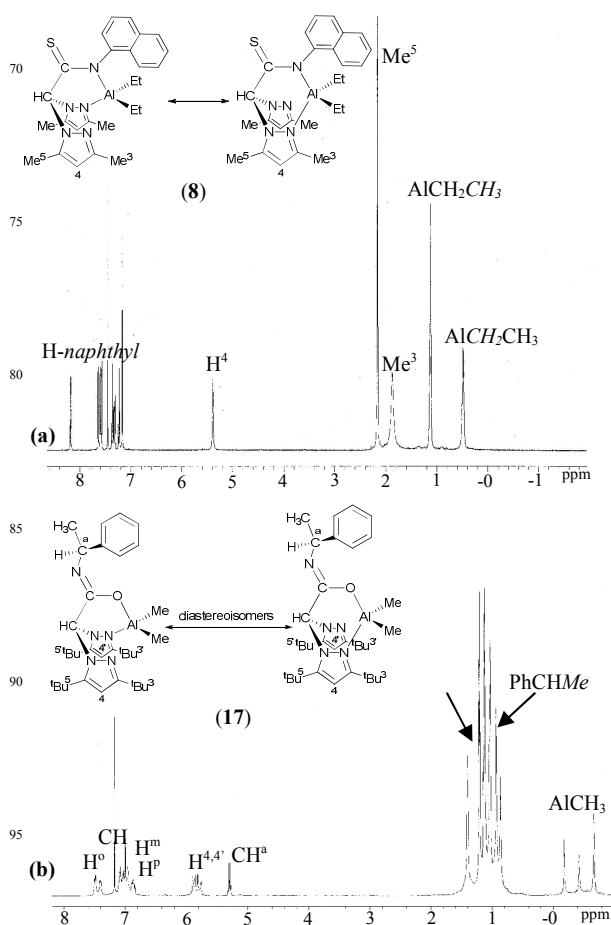


Fig. 2. ¹H NMR spectra at room temperature of [AlEt₂(κ²-nbptam)] (8) (a) and [AlMe₂(κ²-(S)-mtbpbam)] (17) (b) in C₆D₆.

The molecular structure of complex 14 was determined by X-ray diffraction. The ORTEP drawing is depicted in Fig. 3. The crystallographic data and selected interatomic distances and angles are given in Tables S1 and S3 in ESI†. In this complex the heteroscorpionate ligand is κ²NN coordinated to the aluminium centre, thus forming a pseudotetrahedral complex with C₁ symmetry. In addition, the aluminium centre is coordinated to two alkyl ligands.

The solid-state structure is consistent with those proposed in Scheme 2 on the basis of NMR data in solution and other analytical data. Given the coordination mode of the heteroscorpionate ligand, complex **14** is a chiral compound. This complex crystallises as a racemic mixture with both enantiomers included in the unit cell, which belongs to the centrosymmetric space group. The geometry around the aluminium centre can be described as distorted tetrahedral, with the dihedral angle between the N(2)–Al(1)–N(5) and C(37)–Al(1)–C(35) planes (84.25°) consistent with a distorted tetrahedral geometry. Furthermore, the angles around the aluminium atom show considerable deviation from ideal values, in the range 91.5(3)–119.0(17)°, and the most acute angle of 91.5(3)° is observed for N(2)–Al(1)–N(5), which is constrained by the bite of the heteroscorpionate ligand. The distance between N(3) and Al(1) (3.578 Å) is too long to be considered as bonding or as an interaction between N(3) and the Al(1) atom, and it is longer than the distance observed in similar complexes with Me₂-pyrazole rings,^{13c} probably due to the steric hindrance caused by the *tert*-butyl moieties in the pyrazole rings. This steric demand of the *tert*-butyl groups accounts for the Al(1)–N(2) bond distance of 2.015(7) Å is longer than those in Al/Me₂-pyrazolyl complexes.^{13c,17}

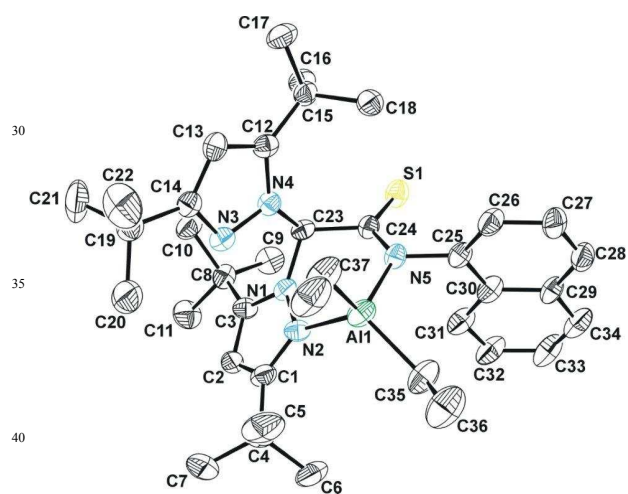


Fig. 3. ORTEP drawing of compound **14**. Thermal ellipsoids are set at 30% probability and hydrogen atoms are omitted for clarity.

Catalytic behaviour in the ROP of bulky heteroscorpionate organoaluminiums

Organoaluminiums **7–18** were tested as initiators for the ROP of cyclic esters. For this purpose ϵ -CL and *rac*-LA were chosen as monomers for polymerisations. In the first screening, compounds **7–18** were tested against ϵ -CL in toluene at 70 °C. It can be seen from the results in Table 1 that organoaluminiums **7–18** are effective initiators for the ROP of ϵ -CL. The activity data compare favourably with those of most discrete aluminium initiators, particularly those related to scorpionate compounds.^{4,13c} Initiators **7–18** proved to be very productive systems and enabled the quantitative conversion of 500 equiv. of ϵ -CL

within minutes at 70 °C (see entries 1–12 in Table 1). Moreover, all of the experimental molecular weights are in good agreement with calculated values and the molecular weight distributions are narrow, both features that are characteristic of a controlled polymerisation. The productivity of these entities and the controlled character of the polymerisation were further evidenced by the sequential polymerisation of 500 + 200 equiv. of ϵ -CL (entry 13), for which complete conversion was observed along with a slight broadening of the molecular weight distribution between the two stages. It is worth noting that an increase in the activity in the ROP of ϵ -CL is produced by the steric hindrance from the *tert*-butyl groups on the bulky heteroscorpionate ligands (see Entries 1 and 2 versus Entries 7 and 8, respectively).

On the basis of the data in Table 1, compound **14** was chosen as the most effective initiator to carry out a more in-depth study of the catalytic behaviour of these systems in ROP (see Entries 14–19 in Table 1). A faster conversion of monomer occurred on increasing the temperature (entries 14 and 15) although an increase in the molecular weight distribution was also observed, probably due to the occurrence of transesterification reactions. The possible competition with monomer molecules during polymerisation could mean that a polar solvent, such as THF, is not appropriate for use in catalytic procedures (see Entry 16 in Table 1). Moreover, a decrease in the loading of initiator from 90 to 70 μ mol, under identical conditions, seems to have a detrimental effect on the productivities in ROP (see Entry 17). Remarkably, significant levels of transfer reactions were not observed when higher [Al]:[CL] ratios were chosen (see Entries 18 and 19). In fact, compound **14** is capable of converting 1000 equiv. of ϵ -CL in a very controlled manner to give high molecular weight polymers with narrow molecular weight distributions (see entry 19 in Table 1).

In order to determine reaction rate constants for the best initiators, solution kinetics studies were carried out on the ROP of ϵ -CL for the thioacetamide derivatives **12** and **14** and the acetamide derivatives **16** and **18**. Polymerisations were monitored over time by regular manual sampling followed by ¹H NMR analysis to determine the degree of monomer conversion. The semi-logarithmic plots of $\ln([CL]_0/[CL]_t)$ versus reaction time for initiators **12**, **14**, **16** and **18** are depicted in Figure 4, where [CL]₀ is the initial ϵ -CL monomer concentration and [CL]_t is the ϵ -CL concentration at a given reaction time *t*. In all cases the linearity of the plots shows a first order with respect to ϵ -CL monomer for polymerisations at 70 °C. An induction period was not observed and this indicates that initiator aggregates were not required to produce active species. The linearity of the plots also shows that termination reactions did not occur during polymerisation. The *k*_{app} values for these derivatives are of the same order of magnitude and are roughly one order higher than the *k*_{app} values found for the Me₂-pyrazole derivatives.^{13c}

Table 1. Screening for the polymerisation of ε -CL by initiators 7–18.

entry	Init	[CL] ₀ /[Al] ₀	time (min)	Conv (%) ^c	$M_n(\text{theor.})$ (Da) ^d	$M_n(\text{exp.})$ (Da) ^e	M_w/M_n
1	7	500	75	94	53645	60400	1.28
2	8	500	70	94	53645	59320	1.31
3	9	500	180	93	53075	59300	1.29
4	10	500	160	95	54217	58130	1.25
5	11	500	60	93	53075	54910	1.13
6	12	500	60	98	55929	56010	1.14
7	13	500	50	93	53075	53850	1.11
8	14	500	45	93	53075	53560	1.13
9	15	500	95	98	55929	56650	1.12
10	16	500	80	94	53645	55870	1.15
11	17	500	65	94	53645	54980	1.14
12	18	500	55	93	53075	55180	1.11
13	14	500 + 200	60	94	75104	81520	1.19
14 ^b	14	500	1440	92	52504	52650	1.07
15 ^b	14	500	5	95	54217	85400	1.46
16 ^f	14	500	120	53	30247	63580	1.55
17 ^g	14	500	120	90	51363	52330	1.09
18	14	200	25	95	21687	23110	1.09
19	14	1000	75	98	111857	124120	1.17

^aPolymerisation conditions: 90 μ mol of initiator, 20 mL of toluene as solvent and at 70 °C of temperature, ^b(entry 14 at 25 °C; entry 15 at 110 °C). ^cPercentage conversion of the monomer [(weight of polymer recovered/weight monomer) \times 100]. ^dTheoretical M_n = (monomer/initiator) \times (% conversion) \times (M_w of ε -CL). ^eDetermined by GPC relative to polystyrene standards in tetrahydrofuran. Experimental M_n was calculated considering Mark–Houwink’s corrections;¹⁸ [$M_n = 0.56 \times M_n(\text{GPC})$]. ^fTHF as solvent. ^g70 μ mol of initiator.

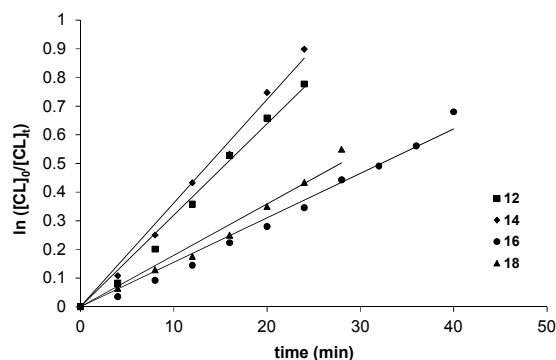


Fig. 4. First-order kinetic plots for ε -CL polymerisations in toluene at 70 °C with [CL]:[Al] = 200 and [Al] = 4.5×10^{-3} mol L⁻¹: ■ **12**, $k_{\text{app}} = 5.32 \times 10^{-4}$ s⁻¹ (linear fit, $R^2 = 0.988$); ● **14**, $k_{\text{app}} = 6.03 \times 10^{-4}$ s⁻¹ (linear fit, $R^2 = 0.990$); ▲ **16**, $k_{\text{app}} = 2.58 \times 10^{-4}$ s⁻¹ (linear fit, $R^2 = 0.978$); ▼ **18**, $k_{\text{app}} = 2.99 \times 10^{-4}$ s⁻¹ (linear fit, $R = 0.978$).

Due to the excellent performance observed for the initiator **14** in the ROP of ε -CL, this organoaluminium was systematically examined for the production of polylactides (PLAs) from *rac*-lactide. Initiator **18** was also tested in order to study the influence of a stereogenic

centre in the molecule that could interfere in the stereoselectivity of the incoming polymers (Table 2). The resulting PLA had a molecular weight in close agreement with the calculated value for one polymer chain per metal centre, and the GPC data for the resulting polyester showed a monomodal weight distribution (see Fig. S4 in ESI†). Thus, initiator **14** gave 87% conversion of 200 equiv. after 7.5 hours and produced a medium-to-high molecular weight material with a very narrow polydispersity (Entry 1 in Table 2). Furthermore, the use of derivative **18** led to the transformation of 56% of the monomer, under otherwise identical conditions, to give a product with a very narrow molecular weight distribution (Entry 4).

Table 2. Polymerisation of *rac*-LA by initiators **14** and **18**.

entry	Init	Temp (°C)	time (h)	Conv (%) ^b	$M_n(\text{theor.})$ (Da) ^c	$M_n(\text{exp.})$ (Da) ^d	M_w/M_n	P_m ^e
1	14	110	7.5	87	25056	25950	1.08	0.49
2	14	90	20	91	26208	26470	1.06	0.52
3	14	70	72	84	24192	23960	1.04	0.50
4	18	110	7.5	56	16128	14950	1.06	0.53
5	18	90	20	78	22464	23120	1.06	0.57
6	18	70	72	40	11520	11140	1.04	0.60

^aPolymerisation conditions: 90 μ mol of initiator, [LA]₀/[Al]₀ = 200, 20 mL of toluene as solvent. ^bPercentage conversion of the monomer [(weight of polymer recovered/weight monomer) \times 100]. ^cTheoretical M_n = (monomer/initiator) \times (% conversion) \times (M_w of ε -CL). ^dDetermined by GPC relative to polystyrene standards in tetrahydrofuran. Experimental M_n was calculated considering Mark–Houwink’s corrections;¹⁸ [$M_n = 0.56 \times M_n(\text{GPC})$]. ^e P_m is the probability of forming a new *m*-dyad.

The polymerisation of *rac*-LA was monitored over time by manual sampling followed by ¹H-NMR analysis to determine the degree of monomer conversion. The polymerisation kinetics were studied for complexes **14** and **18** with [LA]₀/[Al]₀ = 200 and [Al] = 4.5×10^{-3} M at 110 °C, 100 °C, 90 °C, 80 °C and 70 °C, using toluene as solvent. The semi-logarithmic plots of ln([LA]₀/[LA]_t) versus reaction time for both initiators are shown in Figure 5, where [LA]₀ is the initial lactide monomer concentration and [LA]_t is the lactide concentration at a given reaction time *t*. Once again, the linearity of the plot indicates that the propagation was first order with respect to lactide monomer when polymerised in toluene. Furthermore, an induction period was not observed. The fastest polymerisation for *rac*-LA was observed for **14** at 110 °C, which gave a pseudo-first-order rate constant of 2.14×10^{-4} s⁻¹. Finally, the influence of the temperature on the polymerisation rate of *rac*-LA using **14** and **18** was also investigated. It can be seen from Figure 5 that the polymerisation rate increased with increasing temperature. From the five k_{app} values determined at different temperatures, the activation energies of the polymerisations using **14** and **18** were deduced by fitting

$\ln k_{app}$ versus T^{-1} according to the Arrhenius equation (see Fig. 6). The activation energy E_a values for the *rac*-LA polymerisation using **14** and **18** were 6.46 and 6.87 kJ mol⁻¹, respectively. The activation energy for these initiators was much lower when compared to the E_a data for tin(II) ethylhexanoate (70.9 kJ mol⁻¹).¹⁹

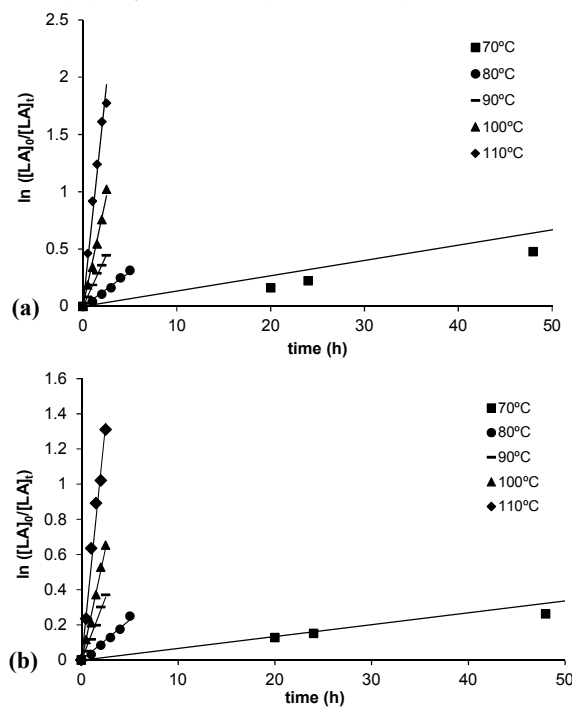


Fig. 5. First-order kinetic plots for initiators **14** and **18** for *rac*-LA polymerisations in toluene with $[LA]_0/[A]_0 = 200$ and $[A]_0 = 4.5 \times 10^{-3}$ mol L⁻¹. (a) **14**, \blacklozenge at 110 °C, $k_{app} = 2.15 \times 10^{-4}$ s⁻¹ (linear fit, $R^2 = 0.973$); \blacktriangle at 100 °C, $k_{app} = 1.07 \times 10^{-4}$ s⁻¹ (linear fit, $R^2 = 0.991$); \blacktriangledown at 90 °C, $k_{app} = 5.03 \times 10^{-4}$ s⁻¹ (linear fit, $R^2 = 0.997$); \bullet at 80 °C, $k_{app} = 1.67 \times 10^{-5}$ s⁻¹ (linear fit, $R^2 = 0.984$); \blacksquare at 70 °C, $k_{app} = 3.72 \times 10^{-6}$ s⁻¹ (linear fit, $R^2 = 0.954$). (b) **18**, \blacklozenge at 110 °C, $k_{app} = 1.50 \times 10^{-4}$ s⁻¹ (linear fit, $R^2 = 0.982$); \blacktriangle at 100 °C, $k_{app} = 7.10 \times 10^{-5}$ s⁻¹ (linear fit, $R^2 = 0.991$); \blacktriangledown at 90 °C, $k_{app} = 3.98 \times 10^{-5}$ s⁻¹ (linear fit, $R^2 = 0.983$); \bullet at 80 °C, $k_{app} = 1.27 \times 10^{-5}$ s⁻¹ (linear fit, $R^2 = 0.980$); \blacksquare at 70 °C, $k_{app} = 1.86 \times 10^{-6}$ s⁻¹ (linear fit, $R^2 = 0.985$).

Microstructural analysis of the polyesters was carried out by ¹H NMR spectroscopy, Size Exclusion Chromatography and MALDI-TOF MS. All of the polymers exhibited a monomodal and narrow molecular weight distribution (see Fig. S4, as an example, in ESI†). The low molecular weight PLA sample obtained with initiator **14** was characterised in order to ascertain the nature of the initiator. It was established by MALDI-TOF (see Fig. S5 in ESI†) and ¹H NMR (see Fig. S6 in ESI†) data that the polymer chains are selectively capped by –COCH₂CH₃ and –OH end groups. This provides evidence that the polymerisation follows a nucleophilic route and is initiated by the transfer of an alkyl ligand to the monomer, with cleavage of the acyl-oxygen bond and formation of a metal alkoxide propagating species. The homonuclear decoupled ¹H NMR spectrum of the methine region of the PLA samples derived from compounds **14** and **18** in toluene is consistent with the formation of chains that are essentially atactic (see Fig. S7 in in ESI† and P_m in Table 2).

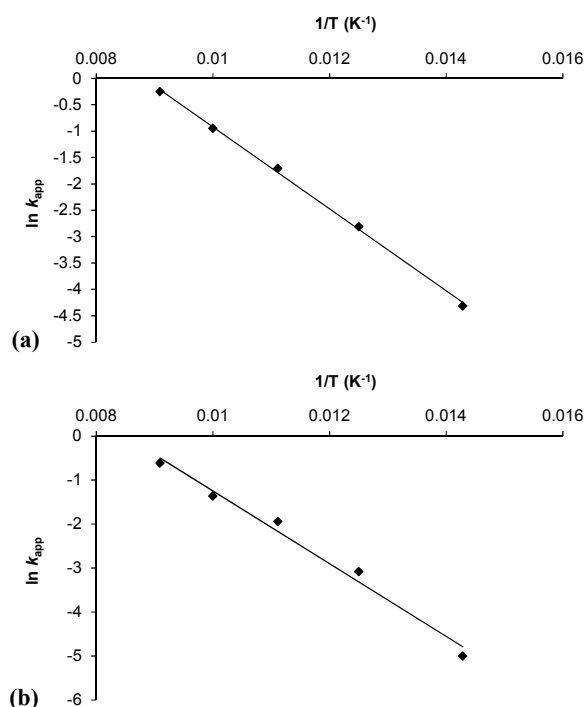
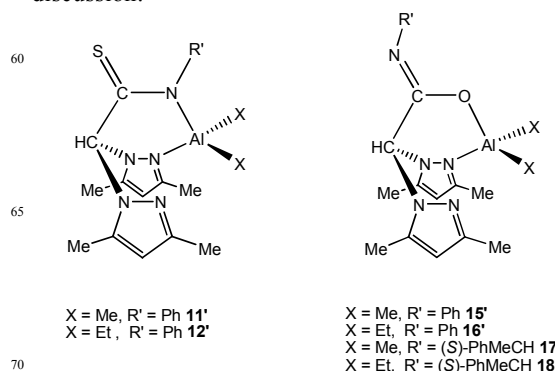


Fig. 6. (a) Plot of $\ln k_{app}$ versus T^{-1} for complex **14** in toluene with $[LA]_0/[A]_0 = 200$ and $[A] = 4.5 \times 10^{-3}$ mol L⁻¹ (linear fit, $R^2 = 0.999$). (b) Plot of $\ln k_{app}$ versus T^{-1} for complex **18** in toluene with $[LA]_0/[A]_0 = 200$ and $[A] = 4.5 \times 10^{-3}$ mol L⁻¹ (linear fit, $R^2 = 0.985$).

Comparative study between *t*-Bu₂-pyrazole and Me₂-pyrazole organoaluminium derivatives in ROP

We were interested in establishing an appropriate comparative discussion of the reactivity of these new initiators with those reported in a previous publication^{13c} with the aim of drawing conclusions about possible improvements in ROP. For this purpose, the structures of the Me₂-pyrazole counterparts are shown in Scheme 3. The compounds previously reported are renumbered on the basis of similarities between them in order to facilitate the discussion.



Scheme 3. Non-bulky heteroscorpionate initiators reported previously.

Nature of the alkyl group

The nature of the alkyl group in both families of initiators (Me₂- and *t*-Bu₂-pyrazole derivatives) seems to affect the catalytic activity, which decreases in the order Et > Me – a

trend that is also consistent with the decrease in the lability of the M–C bond (see as examples entry 1 versus entry 2, and entry 3 versus entry 4 in Table 3 for *t*Bu₂-pyrazole derivatives; and also entry 5 versus 6, and entry 7 versus 8 in Table 3 for Me₂-pyrazole analogues^{13c}). Similar behaviour has also been observed in analogous derivatives.^{13a,13c,20}

Table 3. Polymerisation of ϵ -CL catalysed by alkyl aluminium compounds.

entry	Init	[CL] ₀ /[Al] ₀	time (min)	conv (%) ^b	M_n (theor.) (Da) ^c	M_n (exp.) (Da) ^d	M_w/M_n
1	7	500	75	94	53645	60400	1.28
2	8	500	70	94	53645	59320	1.31
3	13	500	50	93	53075	53850	1.11
4	14	500	45	93	53075	53560	1.13
5 ^{13c}	11'	500	14(h)	95	54150	74780	1.45
6 ^{13c}	12'	500	8(h)	70	39900	45320	1.36
7 ^{13c}	15'	500	4(h)	72	41040	43940	1.32
8 ^{13c}	16'	500	3(h)	84	47880	65736	1.47
9	9	500	180	93	53075	59300	1.29
10	10	500	160	95	54217	58130	1.25

¹⁰ ^aPolymerisation conditions: 90 μ mol of initiator, 20 mL of toluene as solvent at 70 °C. ^bPercentage conversion of the monomer [(weight of polymer recovered/weight monomer) \times 100]. ^cTheoretical M_n = (monomer/initiator) \times (% conversion) \times (M_w of ϵ -CL). ^dDetermined by GPC relative to polystyrene standards in tetrahydrofuran.

¹⁵ Experimental M_n was calculated considering Mark–Houwink's corrections,¹⁸ [$M_n = 0.56 \times M_n$ (GPC)].

Influence of the encumbered substituents in the pyrazole moieties

²⁰ The presence of encumbered substituents in the pyrazole moieties of the aluminium derivatives seems to improve catalytic performance in terms of activity and degree of control. As a first comparison, alkyl aluminium derivatives **11–18** were found to be markedly more active than the analogous Me₂-pyrazole derivatives **11'–12'** and **15'–18'**, which were recently reported by our group. As an example, compound **12** can quantitatively polymerise, in a controlled fashion, 500 equiv. of ϵ -CL in only 60 minutes (see entry 6 in Table 1), whereas compound **12'** requires 8 hours to achieve 70% conversion.^{13c} The *t*Bu₂-pyrazole initiators show reasonably well-controlled behaviour in the ROP of lactones and lactides, giving rise to polymers with excellent consistency between calculated and observed molecular weights (see Table 1 and Table 2). In contrast, derivatives **11'–12'** and **15'–18'** gave rise to polymers with substantially higher molecular weights than those predicted,^{13c} a trend that is consistent with poor rates of initiation (ϵ -CL initiation in the Al–Et bond) compared to propagation.

⁴⁰ The polymers obtained by both families of initiator had a monomodal weight distribution, but the M_w/M_n values for Me₂-pyrazole derivatives are somewhat higher than those expected for a purely living polymerisation, probably due to higher levels of the transesterification side reaction,

45 which would result in the formation of macrocycles with a wider range of molecular weight distributions. The overall results are consistent with a better controlled polymerisation model for *t*Bu₂-pyrazole derivatives, which gave rise to M_w/M_n values between 1.04 and 1.15 (see 50 Tables 1 and 2).

As far as the stereoselectivities in the ROP of *rac*-LA are concerned, the *t*Bu₂-pyrazole derivative **14** (see P_m in entries 1–3 in Table 2) and the counterparts **11'–12'** and **15'–18'** did not have any control over the tacticity of the 55 growing polymer chain, essentially giving rise to atactic polymers. Unexpectedly, and assuming a chain-end mechanism, the high steric demand of the *t*Bu substituents in the two pyrazole rings did not lead to sufficient steric congestion and, as a consequence, did not provide more 60 selective active centres to the incoming lactide. On the other hand, the sterically hindered initiator **18**, which is a mixture of two diastereoisomers, promoted an isotactic bias in the polymerisation of *rac*-LA in toluene at 70 °C to produce slightly enhanced degrees of isotacticity (see P_m 65 in entries 4–6 in Table 2) – albeit with a significant decrease in activity.

Influence of the steric hindrance in the acetamidate/thioacetamidate moiety

⁷⁰ Improvements in catalytic performance were also observed in cases where only the pendant donor arm of the heteroscorpionate ligand was chosen to increase the steric hindrance in the organoaluminium initiators. Thus, the most congested thioacetamidate derivatives **7** and **8** show 75 better catalytic behaviour in the polymerisation of ϵ -CL than their analogues **11'** and **12'**, as do the acetamidate derivatives **9** and **10** with respect to their analogues **15'** and **16'** (Table 3). For instance, compound **10** converts 95% of the monomer in 160 minutes in a controlled 80 fashion, whereas compound **16'** requires three hours to achieve 84% conversion.

Conclusions

Guided by the results of previous studies, in which several 85 organoaluminiums based on heteroscorpionate scaffolds were reported, we focused our efforts on improving the catalytic behaviour of these systems in the ROP of cyclic esters by the introduction of encumbered substituents in the structure. A total of twelve thioacetamidate and 90 acetamidate organoaluminium derivatives with bulky heteroscorpionate ligands were synthesised and fully characterised. These new compounds were tested as initiators in the ROP of ϵ -CL and *rac*-LA. Improvements in productivity and in the control of the polymerisation 95 process were observed. In fact, excellent agreement was found between calculated and observed molecular weights, and polyesters with very narrow polydispersities were obtained with these entities. Among the twelve compounds described, organoaluminium **14**, with bulky 100 substituents in the pyrazole and thioacetamidate moieties, can be highlighted as the most efficient initiator in ROP. Solution kinetic studies for the ROP of ϵ -CL and *rac*-LA

by the best initiators complement the catalytic study and provided values for k_{app} and E_a .

Unexpectedly, the steric hindrance imposed on the structures of the new initiators was not sufficient to control the tacticity of the PLAs obtained by ROP of *rac*-lactide. However, when the polymerisations were carried out with compound **18**, a slightly higher level of isotacticity was obtained and the probability value increased slightly in this case to $P_m = 0.60$. The behaviour observed during the propagation cannot be the result of the high steric demand of the ^tBu substituents in the two pyrazole rings because better control was not obtained with the other bulky heteroscorpionate initiators.

In conclusion, rational tuning of the catalyst design has enabled the preparation of the most efficient catalyst systems for the ROP of cyclic esters. However, further iterations of ligand design will be required to identify organoaluminiums that would be capable of achieving stereochemical control under solution ROP conditions.

Experimental

All manipulations were performed under nitrogen, using standard Schlenk techniques. Solvents were pre-dried over sodium wire (toluene, n-hexane and THF) and distilled under nitrogen from sodium (toluene and THF) or sodium-potassium alloy (n-hexane). Deuterated solvents were stored over activated 4 Å molecular sieves and degassed by several freeze-thaw cycles. Microanalyses were carried out with a Perkin-Elmer 2400 CHN analyzer. ¹H and ¹³C NMR spectra were recorded on a Varian Inova FT-500 spectrometer and referenced to the residual deuterated solvent. The NOESY-1D spectra were recorded on a Varian Inova FT-500 with the following acquisition parameters: irradiation time 2 s and number of scans 256, using standard VARIANT-FT software. Two-dimensional NMR spectra were acquired using standard VARIAN-FT software and processed using an IPC-Sun computer. AlMe₃, AlEt₃ and *rac*-lactide were purchased from Aldrich. ϵ -CL was purchased from Alfa-Aesar. ϵ -CL was dried by stirring over fresh CaH₂ for 48 h, then distilled under reduced pressure and stored over activated 4 Å molecular sieves. *rac*-Lactide was sublimed three times, recrystallised from THF and finally sublimed again prior to use. Phenyl isocyanate, phenyl isothiocyanate, fluorenyl isocyanate, (*S*)-(-)- α -methylbenzyl isocyanate and 1-naphthyl isothiocyanate were purchased from Aldrich or Lancaster. The compounds bis(3,5-dimethylpyrazol-1-yl)methane (bdmpzm) and bis(3,5-*tert*-butylpyrazol-1-yl)methane (bdbpzm) were prepared according to literature procedures.¹⁶ Gel permeation chromatography (GPC) measurements were performed on a Polymer Laboratories PL-GPC-220 instrument equipped with a TSK-GEL G3000H column and an ELSD-LTII light-scattering detector. The GPC column was eluted with THF at 50 °C and 1 mL/min and was calibrated using eight monodisperse polystyrene standards in the range 580–483000 Da. The MALDI-TOF spectra were acquired using a Bruker Autoflex II TOF/TOF spectrometer using DCTB

(*trans*-2-[3-(4-*tert*-butylphenyl)-2-methyl-2-propenylidene]malononitrile) and NaI as matrix and cationisation reagent, respectively. Samples cocrystallised with matrix mixture in a ratio of 100:1 on the probe were ionised in positive reflector mode. External calibration was performed by using Peptide Calibration Standard II (covered mass range: 700–3200 Da) and Protein Calibration Standard I (covered mass range: 5000–17,500 Da).

Synthesis of nbptamH (1)

In a 250 mL Schlenk tube, bdmpzm (2.00 g, 9.79 mmol) was dissolved in dry THF (70 mL) and cooled to –78 °C. A 1.6 M solution of BuⁿLi (6.12 mL, 9.79 mmol) in hexane was added and the solution was stirred for 1 h. The resulting mixture was added dropwise to a cooled (–10 °C) solution of 1-naphthyl isothiocyanate (1.81 g, 9.79 mmol). The reaction mixture was allowed to warm up to ambient temperature and was stirred for 1 h. The product was hydrolyzed with saturated aqueous NH₄Cl (15 mL). The organic layer was extracted, dried over MgSO₄, filtered, and the solvent was removed in vacuo to give the product as a yellow oil, which was triturated with hexane to give the pure product as a yellow solid. Yield: 3.12 g, 82%. Anal. Calcd for C₂₂H₂₃N₅S: C, 67.8; H, 6.0; N, 18.0. Found: C, 67.9; H, 6.2; N, 17.8. ¹H NMR (C₆D₆, 297 K), δ (ppm): 12.87 (brs, 1 H, NaphNHCS), 8.52–6.93 (m, 7 H, NaphNHCS), 8.11 (s, 1 H, CH), 6.95 (s, 2 H, H⁴), 1.88 (s, 6 H, Me³), 1.79 (s, 6 H, Me⁵). ¹³C{¹H}NMR (C₆D₆, 297 K), δ (ppm): 76.7 (CH), 149.2, 140.1 (C^{3or5}), 106.6 (C⁴), 13.4 (Me³), 10.6 (Me⁵), 189.9 (NaphNHCS), 134.5–121.8 (NaphNHCS).

Synthesis of fbpamH (2)

The synthetic procedure was the same as for compound **1**, using bdmpzm (2.00 g, 9.79 mmol), a 1.6 M solution of BuⁿLi (6.12 mL, 9.79 mmol) and fluorenyl isocyanate (2.03 g, 9.79 mmol) to give **2** as a white solid. Yield: 3.38 g, 84%. Anal. Calcd for C₂₅H₂₅N₅O: C, 73.0; H, 6.2; N, 17.0. Found: C, 73.3; H, 6.2; N, 16.8. ¹H NMR (C₆D₆, 297 K), δ (ppm): 10.35 (brs, 1 H, FluNHCO), 7.93–7.10 (m, 7 H, *Ar*-FluNHCO), 6.84 (s, 1 H, CH), 5.90 (s, 2 H, H⁴), 3.87 (s, 2 H, CH₂-FluNHCO), 2.42 (s, 6 H, Me³), 2.27 (s, 6 H, Me⁵). ¹³C{¹H}NMR (C₆D₆, 297 K), δ (ppm): 71.3 (CH), 150.1, 141.4 (C^{3or5}), 107.6 (C⁴), 14.0 (Me³), 11.6 (Me⁵), 162.4 (FluNHCO), 144.0–116.0 (*Ar*-FluNHCO), 37.2 (CH₂-FluNHCO).

Synthesis of ptbptamH (3)

The synthetic procedure was the same as for compound **1**, using bdbpzm (3.65 g, 9.79 mmol), a 1.6 M solution of BuⁿLi (6.12 mL, 9.79 mmol) and phenyl isothiocyanate (1.32 g, 9.79 mmol) to give **3** as a yellow solid. Yield: 4.07 g, 82%. Anal. Calcd for C₃₀H₄₅N₅S: C, 71.0; H, 8.9; N, 13.8. Found: C, 71.1; H, 9.0; N, 13.5. ¹H NMR (C₆D₆, 297 K), δ (ppm): 10.10 (brs, 1 H, PhNHCS), 8.04 (d, 2 H, ³J_{HH} = 7.3 Hz, H^o), 7.07 (t, 2 H, ³J_{HH} = 7.3 Hz, H^m), 6.88 (t, 1 H, ³J_{HH} = 7.3 Hz, H^p), 7.97 (s, 1 H, CH), 6.08 (s, 2 H, H⁴), 1.36 (s, 18 H, ¹Bu⁵), 1.34 (s, 18 H, ¹Bu³). ¹³C{¹H}NMR (C₆D₆, 297 K), δ (ppm): 82.0 (CH), 160.5, 153.2 (C^{3or5}), 102.5 (C⁴), 32.3, 31.9 [C(CH₃)₃, ¹Bu^{3or5}],

30.6 [C(CH₃)₃, ¹Bu³], 30.5 [C(CH₃)₃, ¹Bu⁵], 192.6 (PhNHCS), 139.1 (*Cⁱ*, PhNHCS), 129.1 (*C^m*, PhNHCS), 126.4 (*C^p*, PhNHCS), 122.0 (*C^o*, PhNHCS).

Synthesis of ntbptamH (4)

The synthetic procedure was the same as for compound **1**, using bdtbpmz (3.65 g, 9.79 mmol), a 1.6 M solution of BuⁿLi (6.12 mL, 9.79 mmol) and 1-naphthyl isothiocyanate (1.81 g, 9.79 mmol) to give **4** as a yellow solid. Yield: 4.42 g, 81%. Anal. Calcd for C₃₄H₄₇N₅S: C, 73.2; H, 8.5; N, 12.6. Found: C, 73.9; H, 8.6; N, 13.0. ¹H NMR (C₆D₆, 297 K), δ (ppm): 10.35 (brs, 1 H, NaphNHCS), 8.75–7.10 (m, 7 H, NaphNHCS), 8.11 (s, 1 H, CH), 6.12 (s, 2 H, H⁴), 1.35 (s, 18 H, ¹Bu⁵), 1.34 (s, 18 H, ¹Bu³). ¹³C-{¹H}NMR (C₆D₆, 297 K), δ (ppm): 81.7 (CH), 160.7, 153.0 (C^{3or5}), 103.4 (C⁴), 32.3, 31.8 [C(CH₃)₃, ¹Bu^{3or5}], 30.4 [C(CH₃)₃, ¹Bu³], 30.3 [C(CH₃)₃, ¹Bu⁵], 196.4 (NaphNHCS), 134.3–121.1 (NaphNHCS).

Synthesis of ptbpamH (5)

The synthetic procedure was the same as for compound **1**, using bdtbpmz (3.65 g, 9.79 mmol), a 1.6 M solution of BuⁿLi (6.12 mL, 9.79 mmol) and phenyl isocyanate (1.17 g, 9.79 mmol) to give **5** as a white solid. Yield: 4.28 g, 89%. Anal. Calcd for C₃₀H₄₅N₅O: C, 73.3; H, 9.2; N, 14.2. Found: C, 74.0; H, 8.8; N, 14.4. ¹H NMR (C₆D₆, 297 K), δ (ppm): 7.90 (brs, 1 H, PhNHCO), 7.29 (d, 2 H, ³J_{HH} = 7.2 Hz, H^o), 7.21 (t, 2 H, ³J_{HH} = 7.2 Hz, H^m), 7.00 (t, 1 H, ³J_{HH} = 7.3 Hz, H^p), 6.98 (s, 1 H, CH), 5.88 (s, 2 H, H⁴), 1.24 (s, 18 H, ¹Bu⁵), 1.13 (s, 18 H, ¹Bu³). ¹³C-{¹H}NMR (C₆D₆, 297 K), δ (ppm): 76.6 (CH), 160.7, 153.2 (C^{3or5}), 103.5 (C⁴), 32.3, 31.8 [C(CH₃)₃, ¹Bu^{3or5}], 30.4 [C(CH₃)₃, ¹Bu³], 29.6 [C(CH₃)₃, ¹Bu⁵], 164.9 (PhNHCO), 138.5 (*Cⁱ*, PhNHCO), 130.5 (*C^m*, PhNHCO), 123.4 (*C^p*, PhNHCO), 119.6 (*C^o*, PhNHCO).

Synthesis of (S)-mtbpamH (6)

The synthetic procedure was the same as for compound **1**, using bdtbpmz (3.65 g, 9.79 mmol), a 1.6 M solution of BuⁿLi (6.12 mL, 9.79 mmol) and fluoren-2-yl isocyanate (1.44 g, 9.79 mmol) to give **6** as a white solid. Yield: 4.42 g, 87%. [α]_D²⁵ = 22.9° (c = 0.1, toluene). Anal. Calcd for C₃₂H₄₉N₅O: C, 74.0; H, 9.5; N, 13.5. Found: C, 74.4; H, 9.6; N, 13.3. ¹H NMR (C₆D₆, 297 K), δ (ppm): 6.22 [brs, 1 H, (PhCHCH₃)NHCO], 6.98 (s, 1 H, CH), 7.18–7.40 [m, 5 H, (PhCHCH₃)NHCO], 5.99, 5.85 (s, 2 H, H^{4,4'}), 5.16 [m, 1 H, (PhCHCH₃)NHCO], 1.41 [d, 3 H, ³J_{HH} = 7.3 Hz, (PhCHCH₃)NHCO], 1.35, 1.28 (s, 18 H, ¹Bu^{5,5'}), 1.19, 1.16 (s, 18 H, ¹Bu^{3,3'}). ¹³C-{¹H}NMR (C₆D₆, 297 K), δ (ppm): 76.3 (CH), 160.6, 159.9, 153.0, 152.9 (C^{3,3'or5,5'}), 102.4, 102.1 (C^{4,4'}), 32.3, 32.2, 31.8, 31.6 [C(CH₃)₃, ¹Bu^{3,3'or5,5'}], 30.6, 30.4 [C(CH₃)₃, ¹Bu^{3,3'}], 30.5, 30.3 [C(CH₃)₃, ¹Bu^{5,5'}], 166.0 [(PhCHCH₃)NHCO], 143.6 [*Cⁱ*, (PhCHCH₃)NHCO], 128.6 [*C^m*, (PhCHCH₃)NHCO], 127.1 [(*C^p*, (PhCHCH₃)NHCO), 126.3 [*C^o*, (PhCHCH₃)NHCO], 49.4 [(PhCHCH₃)NHCO], 22.3 [(PhCHCH₃)NHCO].

Synthesis of [AlMe₂{κ²-nbptam}] (7)

In a 250 cm³ Schlenk tube, nbptamH (**1**) (0.97 g, 2.50 mmol) was dissolved in dry toluene (70 mL) and cooled at 0 °C. A solution of AlMe₃ (2M in toluene) (1.25 mL, 2.50 mmol) was added and the mixture was allowed to warm up

to room temperature and stirred during 1 h. The solvent was removed in vacuo to give the product as a yellow oil, which was triturated with hexane (20 mL) to give the pure product as a yellow solid. Yield: 1.02 g, 92%. Anal. Calcd. for C₂₄H₂₈AlN₅S: C, 70.4; H, 8.5; N, 11.4. Found: C, 70.6; H, 8.7; N, 11.1. ¹H NMR (C₆D₆, 297 K), δ 7.45 (s, 1H, CH), 8.25–7.20 (m, 7H, NaphNCS), 5.35 (s, 2H, H⁴), 2.11 (s, 6H, Me³), 1.88 (s, 6H, Me⁵), -0.20 (s, 6H, AlCH₃). ¹³C-{¹H} NMR (C₆D₆, 297 K), δ 195.4 (NaphNCS), 135.0–121.8 (NaphNCS), 149.3, 142.6 (C^{3 or 5}), 107.4 (C⁴), 75.4 (CH), 12.9 (Me³), 10.8 (Me⁵), -8.0 (AlCH₃).

Synthesis of [AlEt₂{κ²-nbptam}] (8)

The synthesis of **8** was carried out in an identical manner to **7**, using nbptamH (**1**) (0.97 g, 2.50 mmol) and AlEt₃ (1M in hexane) (2.50 mL, 2.50 mmol). Yield: 1.03 g, 87%. Anal. Calcd. for C₂₆H₃₂AlN₅S: C, 71.1; H, 8.8; N, 10.9. Found: C, 71.4; H, 8.9; N, 10.9. ¹H NMR (C₆D₆, 297 K), δ 7.45 (s, 1H, CH), 8.20–7.20 (m, 7H, NaphNCS), 5.38 (s, 2H, H⁴), 2.16 (s, 6H, Me³), 1.88 (s, 6H, Me⁵), 1.13 (t, 6H, ³J_{HH} = 7.9 Hz, AlCH₂CH₃), 0.49 (m, 4 H, ³J_{HH} = 7.9 Hz, AlCH₂CH₃). ¹³C-{¹H} NMR (C₆D₆, 297 K), δ 195.8 (NaphNCS), 135.2–124.1 (NaphNCS), 150.7, 144.0 (C^{3 or 5}), 107.5 (C⁴), 75.8 (CH), 13.1 (Me³), 11.1 (Me⁵), 9.4 (AlCH₂CH₃), 0.8 (AlCH₂CH₃).

Synthesis of [AlMe₂{κ²-fbpamH}] (9)

The synthesis of **9** was carried out in an identical manner to **7**, using fbpamH (**2**) (1.02 g, 2.50 mmol) and AlMe₃ (2M in toluene) (1.25 mL, 2.50 mmol). Yield: 1.00 g, 86%. Anal. Calcd. for C₂₇H₃₀AlN₅O: C, 69.4; H, 6.5; N, 15.0. Found: C, 69.9; H, 6.6; N, 14.8. ¹H NMR (C₆D₆, 297 K), δ 6.80 (s, 1H, CH), 7.82–7.02 (m, 7H, Ar-FluNCO), 5.58 (s, 2H, H⁴), 3.55 (s, 2 H, CH₂-FluNCO), 2.16 (s, 6H, Me³), 1.73 (s, 6H, Me⁵), -0.18 (s, 6H, AlCH₃). ¹³C-{¹H} NMR (C₆D₆, 297 K), δ 155.0 (FluNCO), 129.0–119.1 (Ar-FluNCO), 149.8, 143.0 (C^{3 or 5}), 107.8 (C⁴), 71.2 (CH), 36.6 (CH₂-FluNCO), 13.5 (Me³), 11.0 (Me⁵), -4.1 (AlCH₃).

Synthesis of [AlMe₂{κ²-fbpamH}] (10)

The synthesis of **10** was carried out in an identical manner to **7**, using fbpamH (**2**) (1.02 g, 2.50 mmol) and AlEt₃ (1M in hexane) (2.50 mL, 2.50 mmol). Yield: 1.10 g, 89%. Anal. Calcd. for C₂₉H₃₄AlN₅O: C, 70.3; H, 6.9; N, 14.1. Found: C, 70.8; H, 7.1; N, 13.8. ¹H NMR (C₆D₆, 297 K), δ 6.70 (s, 1H, CH), 7.86–7.14 (m, 7H, Ar-FluNCO), 5.41 (s, 2H, H⁴), 3.56 (s, 2 H, CH₂-FluNCO), 2.02 (s, 6H, Me³), 1.96 (s, 6H, Me⁵), 1.40 (t, 6H, ³J_{HH} = 7.9 Hz, AlCH₂CH₃), 0.44 (m, 4 H, ³J_{HH} = 7.9 Hz, AlCH₂CH₃). ¹³C-{¹H} NMR (C₆D₆, 297 K), δ 154.4 (FluNCO), 129.0–119.7 (Ar-FluNCO), 145.4, 137.6 (C^{3 or 5}), 107.7 (C⁴), 71.3 (CH), 36.9 (CH₂-FluNCO), 11.4 (Me³), 8.9 (Me⁵), 8.7 (AlCH₂CH₃), -0.2 (AlCH₂CH₃).

Synthesis of [AlMe₂{κ²-ptbptam}] (11)

The synthesis of **11** was carried out in an identical manner to **7**, using ptbptamH (**3**) (1.27 g, 2.50 mmol) and AlMe₃ (2M in toluene) (1.25 mL, 2.50 mmol). Yield: 1.21 g, 86%. Anal. Calcd. for C₃₂H₅₀AlN₅S: C, 68.2; H, 8.9; N, 12.4. Found: C, 68.7; H, 9.1; N, 12.0. ¹H NMR (C₆D₆, 297

K), δ 8.25 (s, 1H, CH), 7.50 (d, 2H, $^3J_{\text{HH}} = 7.2$ Hz, H^o , PhNCS), 7.20 (t, 2H, $^3J_{\text{HH}} = 7.2$ Hz, H^m , PhNCS), 7.02 (t, 1H, $^3J_{\text{HH}} = 7.2$ Hz, H^p , PhNCS), 6.08 (s, 2H, H^4), 1.39 (s, 18H, $^1\text{Bu}^5$), 1.28 (s, 18H, $^1\text{Bu}^3$), -0.60 (s, 6H, AlCH_3). ^{13}C - $\{^1\text{H}\}$ NMR (C_6D_6 , 297 K), δ 196.2 (PhNCS), 146.8 (C^{ipso} , PhNCS), 160.6, 153.2 (C^3 or 5), 129.2 (C^p , PhNCS), 128.5 (C^o , PhNCS), 127.3 (C^m , PhNCS), 104.5 (C^4), 84.4 (CH), 32.4, 32.3 [$\text{C}(\text{CH}_3)_3$, $^1\text{Bu}^{3\text{or}5}$], 30.5 [$\text{C}(\text{CH}_3)_3$, $^1\text{Bu}^3$], 29.9 [$\text{C}(\text{CH}_3)_3$, $^1\text{Bu}^5$], -8.1 (AlCH_3).

10 Synthesis of [AlEt₂{ κ^2 -ptbptam}] (12)

The synthesis of **12** was carried out in an identical manner to **7**, using ptbptamH (**3**) (1.27 g, 2.50 mmol) and AlEt₃ (1M in hexane) (2.50 mL, 2.50 mmol). Yield: 1.30 g, 88%. Anal. Calcd. for C₃₄H₅₄AlN₅S: C, 69.0; H, 9.2; N, 11.8. Found: C, 69.4; H, 9.3; N, 11.3. ^1H NMR (C_6D_6 , 297 K), δ 8.25 (s, 1H, CH), 7.65 (d, 2H, $^3J_{\text{HH}} = 7.1$ Hz, H^o , PhNCS), 7.24 (t, 2H, $^3J_{\text{HH}} = 7.1$ Hz, H^m , PhNCS), 7.02 (t, 1H, $^3J_{\text{HH}} = 7.1$ Hz, H^p , PhNCS), 6.07 (s, 2H, H^4), 1.49 (s, 18H, $^1\text{Bu}^5$), 1.29 (s, 18H, $^1\text{Bu}^3$), 1.40 (m, 6H, AlCH_2CH_3), 0.15 (m, 4 H, $^3J_{\text{HH}} = 7.9$ Hz, AlCH_2CH_3). ^{13}C - $\{^1\text{H}\}$ NMR (C_6D_6 , 297 K), δ 196.8 (PhNCS), 146.7 (C^{ipso} , PhNCS), 159.6, 151.5 (C^3 or 5), 129.4 (C^p , PhNCS), 128.5 (C^o , PhNCS), 126.9 (C^m , PhNCS), 104.5 (C^4), 84.1 (CH), 32.3, 31.8 [$\text{C}(\text{CH}_3)_3$, $^1\text{Bu}^{3\text{or}5}$], 30.5 [$\text{C}(\text{CH}_3)_3$, $^1\text{Bu}^3$], 29.9 [$\text{C}(\text{CH}_3)_3$, $^1\text{Bu}^5$], 9.4 (AlCH_2CH_3), -0.2 (AlCH_2CH_3).

25 Synthesis of [AlMe₂{ κ^2 -ntbptam}] (13)

The synthesis of **13** was carried out in an identical manner to **7**, using ntbptamH (**4**) (1.39 g, 2.50 mmol) and AlMe₃ (2M in toluene) (1.25 mL, 2.50 mmol). Yield: 1.33 g, 87%. Anal. Calcd. for C₃₆H₅₂AlN₅S: C, 70.4; H, 8.5; N, 11.4. Found: C, 70.6; H, 8.7; N, 11.1. ^1H NMR (C_6D_6 , 297 K), δ 8.28 (s, 1H, CH), 8.06–7.12 (m, 7H, NaphNCS), 6.07 (s, 2H, H^4), 1.49 (s, 18H, $^1\text{Bu}^5$), 1.29 (s, 18H, $^1\text{Bu}^3$), -0.70 (s, 6H, AlCH_3). ^{13}C - $\{^1\text{H}\}$ NMR (C_6D_6 , 297 K), δ 196.8 (NaphNCS), 144.0–121.4 (NaphNCS), 161.0, 153.3 (C^3 or 5), 104.8, 104.5 (C^4), 84.0 (CH), 32.7, 32.6, 32.4, 32.0 [$\text{C}(\text{CH}_3)_3$, $^1\text{Bu}^{3\text{or}5}$], 30.6, 30.5 [$\text{C}(\text{CH}_3)_3$, $^1\text{Bu}^3$], 30.3, 29.9 [$\text{C}(\text{CH}_3)_3$, $^1\text{Bu}^5$], -4.0 (AlCH_3).

35 Synthesis of [AlEt₂{ κ^2 -ntbptam}] (14)

The synthesis of **14** was carried out in an identical manner to **7**, using ntbptamH (**4**) (1.39 g, 2.50 mmol) and AlEt₃ (1M in hexane) (2.50 mL, 2.50 mmol). Yield: 1.43 g, 89%. Anal. Calcd. for C₃₈H₅₆AlN₅S: C, 71.1; H, 8.8; N, 10.9. Found: C, 71.4; H, 8.9; N, 10.9. ^1H NMR (C_6D_6 , 297 K), δ 8.32 (s, 1H, CH), 7.97–7.02 (m, 7H, NaphNCS), 6.12 (s, 2H, H^4), 1.49 (s, 18H, $^1\text{Bu}^5$), 1.25 (s, 18H, $^1\text{Bu}^3$), 1.40 (m, 6H, AlCH_2CH_3), 0.50 (m, 4 H, AlCH_2CH_3). ^{13}C - $\{^1\text{H}\}$ NMR (C_6D_6 , 297 K), δ 197.2 (NaphNCS), 144.4–120.4 (NaphNCS), 159.9, 153.0 (C^3 or 5), 104.9, 102.9 (C^4), 83.6 (CH), 32.7, 32.5 [$\text{C}(\text{CH}_3)_3$, $^1\text{Bu}^{3\text{or}5}$], 30.5 [$\text{C}(\text{CH}_3)_3$, $^1\text{Bu}^3$], 29.7 [$\text{C}(\text{CH}_3)_3$, $^1\text{Bu}^5$], 10.4 (AlCH_2CH_3), 0.4 (AlCH_2CH_3).

50 Synthesis of [AlMe₂{ κ^2 -ptbpam}] (15)

The synthesis of **15** was carried out in an identical manner to **7**, using ptbpamH (**5**) (1.23 g, 2.50 mmol) and AlMe₃ (2M in toluene) (1.25 mL, 2.50 mmol). Yield: 1.18 g, 86%. Anal. Calcd. for C₃₂H₅₀AlN₅O: C, 70.2; H, 9.2; N, 12.8. Found: C, 71.0; H, 8.9 N, 12.5. ^1H NMR (C_6D_6 , 297 K), δ 7.36 (s, 1H, CH), 7.35–7.00 (m, 5H, PhNCO), 6.03

(s, 2H, H^4), 1.25 (s, 18H, $^1\text{Bu}^5$), 1.19 (s, 18H, $^1\text{Bu}^3$), -0.50 (s, 6H, AlCH_3). ^{13}C - $\{^1\text{H}\}$ NMR (C_6D_6 , 297 K), δ 159.8 (PhNCO), 140.2 (C^{ipso} , PhNCO), 149.4, 140.4 (C^3 or 5), 129.5 (C^m , PhNCO), 127.4 (C^p , PhNCO), 126.5 (C^o , PhNCO), 105.0 (C^4), 76.5 (CH), 32.4, 32.3 [$\text{C}(\text{CH}_3)_3$, $^1\text{Bu}^{3\text{or}5}$], 30.5 [$\text{C}(\text{CH}_3)_3$, $^1\text{Bu}^5$], 29.9 [$\text{C}(\text{CH}_3)_3$, $^1\text{Bu}^3$], -6.1 (AlCH₃).

Synthesis of [AlEt₂{ κ^2 -ptbpam}] (16)

The synthesis of **16** was carried out in an identical manner to **7**, using ptbpamH (**5**) (1.23 g, 2.50 mmol) and AlEt₃ (1M in hexane) (2.50 mL, 2.50 mmol). Yield: 1.28 g, 89%. Anal. Calcd. for C₃₄H₅₄AlN₅O: C, 70.9; H, 9.5; N, 12.2. Found: C, 71.5; H, 9.7; N, 12.0. ^1H NMR (C_6D_6 , 297 K), δ 7.46 (s, 1H, CH), 7.79 (d, 2H, $^3J_{\text{HH}} = 7.2$ Hz, H^o , PhNCO), 7.32 (t, 2H, $^3J_{\text{HH}} = 7.2$ Hz, H^m , PhNCO), 7.02 (brs, 1H, H^p , PhNCO), 6.05, 6.01 (s, 2H, $H^{4,4'}$), 1.55, 1.35 (s, 18H, $^1\text{Bu}^{5,5'}$), 1.21, 1.05 (s, 18H, $^1\text{Bu}^{3,3'}$), 1.40–1.10 (m, 6H, AlCH_2CH_3), 0.50–0.00 (m, 4 H, AlCH_2CH_3). ^{13}C - $\{^1\text{H}\}$ NMR (C_6D_6 , 297 K), δ 160.3 (PhNCO), 141.2 (C^{ipso} , PhNCO), 151.8, 151.6, 151.1, 150.3 (C^3 or 5), 128.6 (C^m , PhNCO), 124.9 (C^p , PhNCO), 124.3 (C^o , PhNCO), 103.3, 102.5 (C^4), 76.8 (CH), 32.9, 32.1, 31.8 [$\text{C}(\text{CH}_3)_3$, $^1\text{Bu}^{3\text{or}5}$], 30.7, 30.3 [$\text{C}(\text{CH}_3)_3$, $^1\text{Bu}^5$], 29.7, 29.1 [$\text{C}(\text{CH}_3)_3$, $^1\text{Bu}^3$], 9.4, 9.1 (AlCH_2CH_3), 0.2, -0.4 (AlCH_2CH_3).

Synthesis of [AlMe₂{ κ^2 -(S)-mtbpam}] (17)

The synthesis of **17** (mixture of two diastereoisomers) was carried out in an identical manner to **7**, using mtbpamH (**6**) (1.30 g, 2.50 mmol) and AlMe₃ (2M in toluene) (1.25 mL, 2.50 mmol). Yield: 1.24 g, 86%. $[\alpha]_{\text{D}}^{25} = 9.6^\circ$ ($c = 0.1$, toluene). Anal. Calcd. for C₃₄H₅₄AlN₅O: C, 70.9; H, 9.5; N, 12.2. Found: C, 70.9; H, 9.6; N, 12.0. ^1H NMR (C_6D_6 , 297 K), δ 7.49, 7.40 [d, 4H, $^3J_{\text{HH}} = 7.2$ Hz, H^o , Ph(CH₃)CHNCO], 7.25–6.80 [m, 6H, H^m and H^p , Ph(CH₃)CHNCO], 6.90 (s, 2H, CH), 5.29 [m, 2H, $^3J_{\text{HH}} = 6.2$ Hz, Ph(CH₃)CHNCO], 5.89, 5.85, 5.84, 5.76 (s, 4H, $H^{4,4'}$), 1.40–0.80, (brs, 42H, $^1\text{Bu}^{3,3',5,5'}$ and Ph(CH₃)CHNCO], -0.18, -0.43, -0.67 (s, 12H AlCH_3). ^{13}C - $\{^1\text{H}\}$ NMR (C_6D_6 , 297 K), δ 163.7, 169.5 [Ph(CH₃)CHNCO], 157.8, 156.6, 156.4, 155.8 ($\text{C}^{3,3'}$ or $5,5'$), 143.5 [C^{ipso} , Ph(CH₃)CHNCO], 128.6–124.0 [PhCH(CH₃)NCO], 103.4, 102.9, 102.1 ($\text{C}^{4,4'}$), 75.8, 75.6 (CH), 54.5, 51.1 [Ph(CH₃)CHNCO], 24.4, 23.1 [PhCH(CH₃)NCO], 32.7, 32.6, 31.9, 31.6, 29.8, 29.0 [$\text{C}(\text{CH}_3)_3$, $^1\text{Bu}^{3,3',5,5'}$], 30.6, 30.5, 30.1, 29.9, 29.2, 28.9 [$\text{C}(\text{CH}_3)_3$, $^1\text{Bu}^{3,3',5,5'}$], -4.9, -5.1, -8.2 (AlCH_3).

Synthesis of [AlEt₂{ κ^2 -(S)-mtbpam}] (18)

The synthesis of **18** (mixture of two diastereoisomers) was carried out in an identical manner to **7**, using mtbpamH (**6**) (1.30 g, 2.50 mmol) and AlEt₃ (1M in hexane) (2.50 mL, 2.50 mmol). Yield: 1.40 g, 93%. $[\alpha]_{\text{D}}^{25} = 7.8^\circ$ ($c = 0.1$, toluene). Anal. Calcd. for C₃₆H₅₈AlN₅O: C, 71.6; H, 9.7; N, 11.6. Found: C, 72.3; H, 9.8; N, 11.2. ^1H NMR (C_6D_6 , 297 K), δ 7.69, 7.62 [d, 4H, $^3J_{\text{HH}} = 7.2$ Hz, H^o , Ph(CH₃)CHNCO], 7.22–7.12 [m, 6H, H^m and H^p , Ph(CH₃)CHNCO], 7.08 (s, 2H, CH), 5.58 [m, 2H, $^3J_{\text{HH}} = 6.2$ Hz, Ph(CH₃)CHNCO], 6.03, 6.01, 5.98, 5.93 (s, 4H, $H^{4,4'}$), 1.60–0.80, (brs, 42H, $^1\text{Bu}^{3,3',5,5'}$ and Ph(CH₃)CHNCO], 1.60–0.80, (brs, 12H, AlCH_2CH_3),

0.65–0.00 (m, 8 H, AlCH_2CH_3). ^{13}C - $\{^1\text{H}\}$ NMR (C_6D_6 , 297 K), δ 164.8, 164.7 [$\text{Ph}(\text{CH}_3)\text{CHNCO}$], 158.8, 158.7, 158.0, 157.8, 153.6, 153.5, 153.2, 152.9 ($\text{C}^{3,3'}$ or $^{5,5'}$), 143.8 [C^{ipso} , $\text{Ph}(\text{CH}_3)\text{CHNCO}$], 128.6–126.3 [$\text{PhCH}(\text{CH}_3)\text{NCO}$], 103.7, 103.0, 102.3, 102.1 ($\text{C}^{4,4'}$), 76.7, 76.3 (CH), 54.6, 49.3 [$\text{Ph}(\text{CH}_3)\text{CHNCO}$], 24.8, 22.2 [$\text{PhCH}(\text{CH}_3)\text{NCO}$], 32.9, 32.8, 32.3, 31.9, 31.8, 31.7 [$\text{C}(\text{CH}_3)_3$, $^1\text{Bu}^{3,3',5,5'}$], 30.8, 30.6, 30.5, 30.0, 29.5, 29.4, 29.2 [$\text{C}(\text{CH}_3)_3$, $^1\text{Bu}^{3,3',5,5'}$], 4.5, 2.1 (AlCH_2CH_3), 0.8, 0.6 (AlCH_2CH_3).

10 General procedure for solution polymerisation of ε -CL and *rac*-LA

Polymerisations of ε -CL were carried out on a Schlenk line in a dried Schlenk flask equipped with a magnetic stirrer. In a typical procedure, the initiator was dissolved in the appropriate amount of solvent and temperature equilibration was ensured by stirring the solution for 15 min in a temperature-controlled bath. ε -CL was injected and polymerisation times were measured from that point. Polymerisations were terminated by addition of acetic acid (5 vol-%) in methanol. Polymers were precipitated in methanol, filtered, dissolved in THF, reprecipitated in methanol, and dried in vacuo to constant weight. Polymerisations of *rac*-LA were performed on a Schlenk line in a flame-dried Schlenk flask equipped with a magnetic stirrer. The Schlenk tubes were charged in the glovebox with the required amount of *rac*-LA and initiator, separately, and then attached to the vacuum line. The initiator and monomer were dissolved in the appropriate amount of solvent, and temperature equilibration was ensured in both Schlenk flasks by stirring the solutions for 15 min in a bath. The appropriate amount of initiator was added by syringe and polymerisation times were measured from that point. Polymerisations were stopped by injecting a solution of acetic acid (5 vol-%) in methanol. Polymers were precipitated in methanol, filtered, dissolved in THF, reprecipitated in methanol, and dried in vacuo to constant weight.

Polymerisation kinetics

Kinetic experiments were carried out in flasks at 100 °C on the Schlenk line using stock solutions of the reagents. Specifically, at appropriate time intervals a sample was removed by syringe and quickly quenched into 1 mL vials containing 0.6 mL of undried 'wet' CDCl_3 . The quenched aliquots were analyzed by ^1H NMR spectroscopy. For *rac*-LA polymerisation, the $[\text{LA}]_0/[\text{LA}]_t$ ratio was determined by integration of the peaks for LA (5.0 ppm for the methine proton signal) and PLA (5.2 ppm for the methine proton signal) according to the equation $[\text{LA}]_0/[\text{LA}]_t = (A_{5.0} + A_{5.2})/A_{5.0}$. Apparent rate constants (k_{app}) were extracted from the slopes of the best-fit lines to the plots of $\ln([\text{LA}]_0/[\text{LA}]_t)$ versus time. For ε -CL polymerisation, the $[\text{CL}]_0/[\text{CL}]_t$ ratio was determined by integration of the peaks for CL (4.2 ppm for the $\text{CH}_2\text{-O}$ proton signal) and PCL (4.0 ppm for the $\text{CH}_2\text{-O}$ proton signal) according to the equation $[\text{CL}]_0/[\text{CL}]_t = (A_{4.2} + A_{4.0})/A_{4.2}$. Apparent rate constants (k_{app}) were extracted from the slopes of the best-fit lines to the plots of $\ln([\text{CL}]_0/[\text{CL}]_t)$ versus time.

60 X-ray crystallographic structure determination

X-ray crystallography: A summary of crystal data collection and refinement parameters for all compounds is given in Table S1.

The single crystals of **3**, **5** and **14** were mounted on a glass fibre and transferred to a Bruker X8 APEX II CCD-based diffractometer equipped with a graphite monochromated Mo-K α radiation source ($\lambda = 0.71073$ Å). Data were integrated using SAINT²¹ and an absorption correction was performed with the program SADABS.²² The software package SHELXTL version 6.10²³ was used for space group determination, structure solution and refinement by full-matrix least-squares methods based on F^2 . All non-hydrogen atoms were refined with anisotropic thermal parameters except those involved in the disordered groups. The three compounds show disorder for ^1Bu or Et groups. Restraints DELU and SIMU were used for to make the ADP values of the disordered atoms more reasonable but, finally, for **3** and **5** a better result was obtained when they were refined isotropically. Hydrogen atoms were placed using a 'riding model' and included in the refinement at calculated positions. For compound **14**, only crystals of low quality ($R_{\text{int}} = 0.21$) that were very weakly diffracting could be grown but the data were of sufficient quality to determine the molecular and the crystal structure.

Acknowledgments

We gratefully acknowledge financial support from the Ministerio de Economía y Competitividad (MINECO), Spain (Grant No. CTQ2011-22578).

90 Notes and references

^aDepartamento de Química Inorgánica, Orgánica y Bioquímica-Centro de Innovación en Química Avanzada (ORFEO-CINQA), Facultad de Ciencias y Tecnologías Químicas, Universidad de Castilla-La Mancha, 13071-Ciudad Real, Spain. Fax: +34926295318 Tel: +34926295300. E-mail: Antonio.Otero@uclm.es and Agustin.Lara@uclm.es

^bDepartamento de Química Inorgánica, Orgánica y Bioquímica, Facultad de Farmacia, Universidad de Castilla-La Mancha, 02071-Albacete, Spain.

^cDepartamento de Química Inorgánica, Orgánica y Bioquímica, Universidad de Castilla-La Mancha, Escuela Técnica Superior de Ingenieros Industriales, 13071 Ciudad Real, Spain.

[†] Electronic Supplementary Information (ESI) available: Figures and tables giving experimental details. Details of data collection and refinement for complexes **3**, **5** and **14**. CCDC reference numbers 1033053- 1033054- 1033055

- (a) M. A. Woodruff and D. W. Huttmacher, *Prog. Polym. Sci.* 2010, **35**, 1217–1256; (b) A. Duda and S. Penzack, *In Polymers from Renewable Resources: Biopolyesters and Biocatalysis*; C. Scholz, R. A. Gross, Eds.; ACS Symposium Series; American Chemical Society: Washington, DC, 2000; Vol. 764, p. 16; (c) A. Corma, S. Iborra and A. Veltz, *Chem. Rev.*, 2007, **107**, 2411–250; (d) S. W. Shalaby and K. J. L. Burg, editors. *Absorbable and Biodegradable Polymers (Advances in Polymeric Materials)*, Boca Raton: CRC Press; 2003.
- (a) P. Dubois, O. Coulembier and J.-M. Raquez, *In Handbook of Ring-Opening Polymerisation*; Wiley-VCH: Weinheim, 2000; (b) C. A. Wheaton, P. G. Hayes and B. J. Ireland, *Dalton Trans.*, 2009, 4832–4846; (c) C. K. Williams, *Chem. Soc. Rev.*, 2007,

- 36, 1573–1580; (d) J. Wu, T.-L. Yu, C.-T. Chen and C.-C. Lin, *Coord. Chem. Rev.*, 2006, **250**, 602–626; (e) O. Dechy-Cabaret, B. Martin-Vaca and D. Bourissou, *Chem. Rev.*, 2004, **104**, 6147–6176.
- 3 (a) W. H. Wong and D. J. Mooney, in *Synthetic Biodegradable Polymer Scaffolds*, ed. A. Atala and D. J. Mooney, Birkhauser, Boston, 1997; (b) M. H. Hartmann, in *Biopolymers from Renewable Resources*, ed. D. L. Kaplan, Springer, Berlin, 1998, ch. 15, pp. 367–411.
- 10 4 See as recent examples: (a) H. S. Reisberg, H. J. Hurley, R. T. Mathers, J. M. Tanski and Y. D. Y. L. Getzler, *Macromolecules*, 2013, **46**, 3273–3279; (b) F. Hild, L. Brelot and S. Dagorne, *Organometallics*, 2011, **30**, 5457–5462; (c) A. D. Schwarz, Z. Chu and P. Mountford, *Organometallics*, 2010, **29**, 1246–1260; (d) M.-H. Thibault and F.-G. Fontaine, *Dalton Trans.*, 2010, **39**, 5688–5697; (e) N. Iwasa, S. Katao, J. Liu, M. Fujiki, Y.; Furukawa and K. Nomura, *Organometallics*, 2009, **28**, 2179–2188; (f) M. Haddad, M. Laghzaoui, R. Welter and S. Dagorne, *Organometallics*, 2009, **28**, 4584–4592.
- 20 5 See as recent examples: (a) H. Xie, Z. Mou, B. Liu, P. Li, W. Rong, S. Li and D. Cui *Organometallics*, 2014, **33**, 722–730; (b) A. Garcés, L. F. Sánchez-Barba, J. Fernández-Baeza, A. Otero, M. Honrado, A. Lara-Sánchez and A. M. Rodríguez, *Inorg. Chem.*, 2013, **52**, 12691–12701; (c) V. Poirier, T. Roisnel, J.-F. Carpentier and Y. Sarazin, *Dalton Trans.*, 2009, 9820–9827; (d) M.-Y. Shen, Y.-L. Peng, W.-C. Hung and C.-C. Lin, *Dalton Trans.*, 2009, 9906–9913.
- 25 6 See as recent examples: (a) I. Hong and E. Y.-X. Chen, *Macromolecules*, 2014, **47**, 3614–3624; (b) C. Yao, D. Liu, P. Li, C. Wu, S. Li, B. Liu and D. Cui, *Organometallics*, 2014, **33**, 684–691; (c) K. Nie, W. Gu, Y. Yao, Y. Zhang and Q. Shen, *Organometallics*, 2013, **32**, 2608–2617; (d) C. E. Hayes, Y. Sarazin, J.-F. Carpentier, M. J. Katz and D. B. Leznoff, *Organometallics*, 2013, **32**, 1183–1192; (e) A. Otero, J. Fernández-Baeza, A. Lara-Sánchez, C. Alonso-Moreno, I. Márquez-Segovia, L. F. Sánchez-Barba and A. M. Rodríguez, *Angew. Chem. Int. Ed.*, 2009, **48**, 2176–2179.
- 30 7 See as recent examples: (a) A. Stopper, K. Press, J. Okuda, I. Goldberg and M. Kol, *Inorg. Chem.*, 2014, **53**, 9140–9150; (b) N. Maudoux, T. Roisnel, J.-F. Carpentier, Y. Sarazin, *Organometallics*, 2014, **33**, 5740–5748; (c) A. Otero, J. Fernández-Baeza, L. F. Sánchez-Barba, J. Tejada, M. Honrado, A. Garcés, A. Lara-Sánchez and A. M. Rodríguez, *Organometallics*, 2012, **31**, 4191–4202; (d) C. Alonso-Moreno, A. Antiñolo, J. C. García-Martínez, S. García-Yuste, I. López-Solera, A. Otero, J. C. Pérez-Flores and M. T. Tercero-Morales, *Eur. J. Inorg. Chem.*, 2012, 1139–1144.
- 35 8 R. M. Izatt, S. R. Izatt, R. L. Bruening, N. E. Izatt and B. A. Moyer, *Chem. Soc. Rev.* 2014, **43**, 2451–2475.
- 40 9 (a) X. H. Cai and B. Xie, *ARKIVOC*, 2014, 205–248; (b) J. Koller and R. G. Bergman, *Organometallics*, 2010, **29**, 5946–5952.
- 45 10 W. Kaminsky and H. Sinn, *Advances in Polymer Science*, Volume 258, 2013, pp 1–28.
- 50 11 See as recent examples: (a) C. Beattie and M. North, *Chem.–Eur. J.*, 2014, **20**, 8182–8188; (b) J. A. Castro-Osma, C. Alonso-Moreno, A. Lara-Sánchez, J. Martínez, M. North and A. Otero, *Catal. Sci. Technol.*, 2014, **4**, 1674–1684; (c) S. H. Kim, D. Ahn, M. J. Go, M. H. Park, M. Kim, J. Lee and Y. Kim, *Organometallics*, 2014, **33**, 2770–2775; (d) C. J. Whiteoak, N. Kielland, V. Laserna, F. Castro-Gómez, E. Martin, E. C. Escudero-Adán, C. Bo and A. W. Kleij, *Chem.–Eur. J.*, 2014, **20**, 2264–2275. (e) C. J. Whiteoak, N. Kielland, V. Laserna, F. Castro-Gomez, E. Martin, E. C. Escudero-Adan, C. Bo and A. W. Kleij, *ChemInform*. 2014, **45**, DOI. 10.1002/chin.201432141.
- 55 65 (f) C. J. Whiteoak, N. Kielland, V. Laserna, E. C. Escudero-Adán, E. Martin and A. W. Kleij, *J. Am. Chem. Soc.*, 2013, **135**, 1228–1231. (g) J. A. Castro-Osma, A. Lara-Sánchez, M. North, A. Otero and P. Villuendas, *Catal. Sci. Technol.*, 2012, **2**, 1021–1026. (h) C. Chatterjee and M. H. Chisholm, *Inorg. Chem.* 2011, **50**, 4481–4492.
- 60 12 See as examples: (a) M. Honrado, A. Otero, J. Fernández-Baeza, L. F. Sánchez-Barba, A. Garcés, A. Lara-Sánchez and A. M. Rodríguez, *Organometallics*, 2014, **33**, 1859–1866; (b) A. Otero, J. Fernández-Baeza, A. Lara-Sánchez and L. F. Sánchez-Barba, *Coord. Chem. Rev.*, 2013, **257**, 1806–1868; (c) M. Honrado, A. Otero, J. Fernández-Baeza, L. F. Sánchez-Barba, A. Lara-Sánchez, J. Tejada, M. P. Carrión, J. Martínez-Ferrer, A. Garcés and A. M. Rodríguez, *Organometallics*, 2013, **32**, 3437–3440; (d) A. Otero, A. Lara-Sánchez, J. Fernández-Baeza, C. Alonso-Moreno, I. Márquez-Segovia, L. F. Sánchez-Barba, J. A. Castro-Osma and A. M. Rodríguez, *Dalton Trans.*, 2011, **40**, 4687–4696.
- 75 80 13 (a) J. A. Castro-Osma, C. Alonso-Moreno, A. Otero, A. Lara-Sánchez, J. Fernández-Baeza, A. M. Rodríguez, L. F. Sánchez-Barba and J. C. García-Martínez, *Dalton Trans.*, 2013, **42**, 9325–9337; (b) J. A. Castro-Osma, C. Alonso-Moreno, J. C. García-Martínez, J. Fernández-Baeza, L. F. Sánchez-Barba, A. Lara-Sánchez and A. Otero, *Macromolecules*, 2013, **46**, 6388–6394; (c) A. Otero, A. Lara-Sánchez, J. Fernández-Baeza, C. Alonso-Moreno, J. A. Castro-Osma, I. Márquez-Segovia, L. F. Sánchez-Barba, A. M. Rodríguez and J. C. García-Martínez, *Organometallics*, 2011, **30**, 1507–1522.
- 85 90 14 (a) J. F. Dunne, K. Manna, J. W. Wiench, A. Ellern, M. Pruski and A. D. Sadow, *Dalton Trans.*, 2010, **39**, 641–653; (b) M. Shen, W. Zhang, K. Nomura and W.-H. Sun, *Dalton Trans.*, 2009, 9000–9009; (c) H. Du, X. Pang, H. Yu, X. Zhuang, X. Chen, D. Cui, X. Wang and X. Jing, *Macromolecules*, 2007, **40**, 1904–1913; (d) R.-C. Yu, C.-H. Hung, J.-H. Huang, H.-Y. Lee and J.-T. Chen, *Inorg. Chem.*, 2002, **41**, 6450–6455; (e) D. Chakraborty and E. Y.-X. Chen, *Organometallics*, 2002, **21**, 1438–1442.
- 95 100 15 (a) A. Otero, A. Lara-Sánchez, J. Fernández-Baeza, E. Martínez-Caballero, I. Márquez-Segovia, C. Alonso-Moreno, L. F. Sánchez-Barba, A. M. Rodríguez and I. López-Solera, *Dalton Trans.*, 2010, **39**, 930–940; (b) N. G. Spiropoulos, G. C. Chingas, M. Sullivan, J. T. York and E. C. Brown, *Inorg. Chim. Acta*, 2011, **376**, 562–573.
- 105 16 (a) J. Sebastian, P. Sala, J. Del Mazo, M. Sancho, C. Ochia, J. Elguero, J. P. Fayet and M. C. Vertut, *Heterocycl. Chem.*, 1982, **19**, 1141–1145; (b) E. Diez-Barra, A. de la Hoz, A. Sánchez-Migallon and J. Tejada, *J. Chem. Soc., Perkin Trans.*, 1993, **1**, 1079–1083; (c) A. Beck, B. Weibert, N. Burzlaff, *Eur. J. Inorg. Chem.*, 2001, 521–527.
- 110 17 (a) J. Koller and G. Bergman, *Organometallics*, 2012, **31**, 2530–2533; (b) M. H. Chisholm, N. W. Eilerts and J. C. Huffman, *Inorg. Chem.*, 1996, **35**, 445–450; (c) S. Milione, F. Grisi, R. Centore and A. Tuzi, *Organometallics*, 2006, **25**, 266–274.
- 115 18 I. Baraki, P. Dubois, R. Jérôme, P. Teyssie, *J. Polym. Sci., Part A: Polym. Chem.* 1993, **31**, 505–514.
- 120 19 D. R. Witzke, R. Narayan and J. J. Kolstad, *Macromolecules*, 1997, **30**, 7075–7085.
- 125 20 (a) L. F. Sánchez-Barba, A. Garcés, M. Fajardo, C. Alonso-Moreno, J. Fernández-Baeza, A. Otero, A. Antiñolo, J. Tejada, A. Lara-Sánchez and M. I. López-Solera, *Organometallics*, 2007, **26**, 6403–6411; (b) C. Alonso-Moreno, A. Garcés, L. F. Sánchez-Barba, M. Fajardo, J. Fernández-Baeza, A. Otero, A. Antiñolo, A. Lara-Sánchez, L. Broomfield, I. Lopez-Solera and A. M. Rodríguez, *Organometallics*, 2008, **27**, 1310–1321; (c) L. F. Sánchez-Barba, C. Alonso-Moreno, A. Garcés, M. Fajardo, J. Fernández-Baeza, A. Otero, A. Lara-Sánchez, A. M. Rodríguez and I. López-Solera, *Dalton Trans.*, 2009, 8054–8062.
- 130 21 SAINT+ v7.12a. Area-Detector Integration Program. Bruker-Nonius AXS. Madison, Wisconsin, USA, 2004.
- 135 22 G. M. Sheldrick, SADABS version 2004/1. A Program for Empirical Absorption Correction. University of Göttingen, Göttingen, Germany, 2004.
- 23 SHELXTL-NT version 6.12. Structure Determination Package. Bruker-Nonius AXS. Madison, Wisconsin, USA, 2001.